

# Synthesis, Structure, and Ring-Opening Polymerization (ROP) of a Phosphonium-Bridged [1]Ferrocenophane

Timothy J. Peckham, Alan J. Lough, and Ian Manners\*

Department of Chemistry, University of Toronto, 80 St. George Street,  
Toronto M5S 3H6, Ontario, Canada

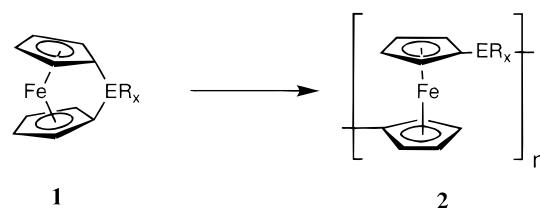
Received August 17, 1998

The stable phosphonium-bridged [1]ferrocenophane  $[(\eta\text{-C}_5\text{H}_4)_2\text{FePPhMe}][\text{OTf}]$  (**10b**) was synthesized by the reaction of the phosphorus-bridged [1]ferrocenophane  $(\eta\text{-C}_5\text{H}_4)_2\text{FePPh}$  (**3a**) with methyl triflate (MeOTf). A single-crystal X-ray diffraction study of **10b** revealed an angle of  $24.4(5)^\circ$  between the planes of the cyclopentadienyl rings, less than the respective angle ( $26.7^\circ$ ) for **3a**. Compound **10b** and a number of other tetracoordinate, phosphorus-bridged [1]ferrocenophanes,  $(\eta\text{-C}_5\text{H}_4)_2\text{FeP(S)Ph}$  (**5a**),  $(\eta\text{-C}_5\text{H}_4)_2\text{FeP}[\text{Fe}(\text{CO})_4]\text{Ph}$  (**6**), and  $[(\eta\text{-C}_5\text{H}_4)_2\text{FePfpPh}][\text{PF}_6]$  (**7**) (where Fp =  $(\eta\text{-C}_5\text{H}_5)\text{Fe}(\text{CO})_2$ ), were investigated with respect to their ring-opening polymerization (ROP) behavior. Only compound **10b** was found to undergo ROP, which occurred both thermally and in the presence of a transition-metal catalyst (PtCl<sub>2</sub>). The resultant ionomeric polymer  $\{[(\eta\text{-C}_5\text{H}_4)_2\text{FePPhMe}][\text{OTf}]\}_n$  (**11**) was found to be soluble in dimethylformamide (DMF), dimethyl sulfoxide (DMSO), methanol, and acetone but displayed only limited stability in these solvents. The thermally ring-opened polymer was found to possess a glass transition temperature of  $176^\circ\text{C}$  and was thermally stable to weight loss up to ca.  $400^\circ\text{C}$ . Analysis by wide-angle X-ray scattering (WAXS) revealed that the polymer was amorphous. A study on the partial to full methylation of the polymer  $[(\eta\text{-C}_5\text{H}_4)_2\text{FePPh}]_n$  (**14**) gave results that were consistent with those from the ROP of **10b**. Dynamic light scattering studies on polymer **11** produced via thermal ROP and transition-metal-catalyzed ROP gave hydrodynamic radii in the range of 30–45 nm, which suggested that the compounds were polymeric rather than oligomeric in nature. On the basis of the glass transition temperatures for a series of samples of polymers **11** of known molecular weight with varying numbers of repeat units (from 20 to 100), the molecular weight ( $M_n$ ) of the transition-metal-catalyzed ROP product was greater than 46 000 (ca. 100 repeat units) and the molecular weight of the thermally produced polymer was even higher.

## Introduction

Transition-metal-containing polymers remain an area of active research due to the potential for obtaining materials with possibly useful physical or catalytic properties that are not easily obtainable with most organic polymer systems.<sup>1–3</sup> We have previously shown that ring-opening polymerization (ROP) of strained [1]-ferrocenophanes (**1**) represents a general route to high-molecular-weight poly(ferrocenes) (**2**).<sup>4–11</sup> The polymerization behavior of the silicon-bridged monomers **1** ( $\text{ER}_x = \text{SiRR}'$ ) is particularly well-developed with a variety of possible substituents at silicon, and thermal, anionic, and transition-metal-catalyzed ROP routes to the interesting polymers **2** ( $\text{ER}_x = \text{SiRR}'$ ) are all known.<sup>4–6,11–13</sup>

The ROP behavior of phosphorus-bridged [1]ferrocenophanes (**3a**) has also been studied. Thus, thermal



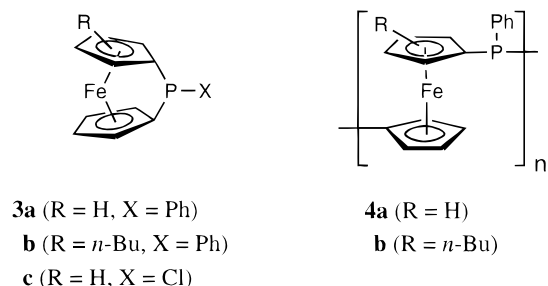
E = Si, Ge, Sn, S, B, etc.

ROP of **3a,b** to afford polymers **4a,b** was reported by our group in 1995.<sup>10</sup> More recently, we have also

(1) (a) Pittman, C. U.; Carraher, C. E.; Reynolds, J. R In *Encyclopedia of Polymer Science and Engineering*; Mark, H. F., Bikales, N. M., Overberger, C. G., Menges, G., Eds.; Wiley: New York, 1989; Vol. 10, p 541. (b) Sheats, J. E.; Carraher, C. E.; Pittman, C. U.; Zeldin, M.; Currell, B. *Inorganic and Metal-Containing Polymeric Materials*; Plenum: New York, 1989. (c) Gonsalves, K. E.; Rausch, M. D. In *Inorganic and Organometallic Polymers*; ACS Symposium Series 360; Zeldin, M., Wynne, K., Allcock, H. R., Eds.; American Chemical Society: Washington, DC, 1988. (d) Allcock, H. R. *Adv. Mater.* **1994**, *6*, 106. (e) Manners, I. *Chem. Br.* **1996**, *32*, 46.

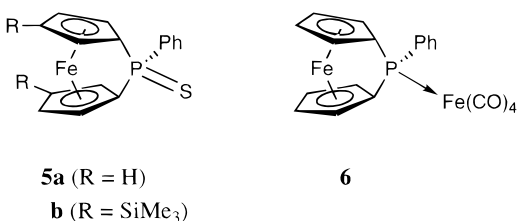
(2) (a) Wright, M. E.; Sigman, M. S. *Macromolecules* **1992**, *25*, 6055. (b) Davies, S. J.; Johnson, B. F. G.; Khan, M. S.; Lewis, J. *J. Chem. Soc., Chem. Commun.* **1991**, 187. (c) Tenhaeff, S. C.; Tyler, D. R. *J. Chem. Soc., Chem. Commun.* **1989**, 1459. (d) Neuse, E. W.; Bednarik, L. *Macromolecules* **1979**, *12*, 187. (e) Brandt, P. F.; Rauchfuss, T. B. *J. Am. Chem. Soc.* **1992**, *114*, 1926. (f) Sturge, K. C.; Hunter, A. D.; McDonald, R.; Santarsiero, B. D. *Organometallics* **1992**, *11*, 3056. (g) Gonsalves, K.; Zhan-ru, L.; Rausch, M. D. *J. Am. Chem. Soc.* **1984**, *106*, 3862. (h) Katz, T. J.; Sudhakar, A.; Teasley, M. F.; Gilbert, A. M.; Geiger, W. E.; Robben, M. P.; Wuensch, M.; Ward, M. D. *J. Am. Chem. Soc.* **1993**, *115*, 3182. (i) Nugent, H. M.; Rosenblum, M. *J. Am. Chem. Soc.* **1993**, *115*, 3848. (j) Patterson, W. J.; McManus, S. P.; Pittman, C. U. *J. Polym. Sci.: Polym. Chem. Ed.* **1974**, *12*, 837. (k) Buretea, M. A.; Tilley, T. D. *Organometallics* **1997**, *16*, 1507. (l) Stanton, C. E.; Lee, T. R.; Grubbs, R. H.; Lewis, N. S.; Pudelski, J. K.; Callstrom, M. R.; Erickson, M. S.; McLaughlin, M. L. *Macromolecules* **1995**, *28*, 8713. (m) Heo, R. W.; Somoza, F. B.; Lee, T. R. *J. Am. Chem. Soc.* **1998**, *120*, 1621.

reported that high-molecular-weight poly(ferrocenylphosphines) and related block copolymers can be obtained



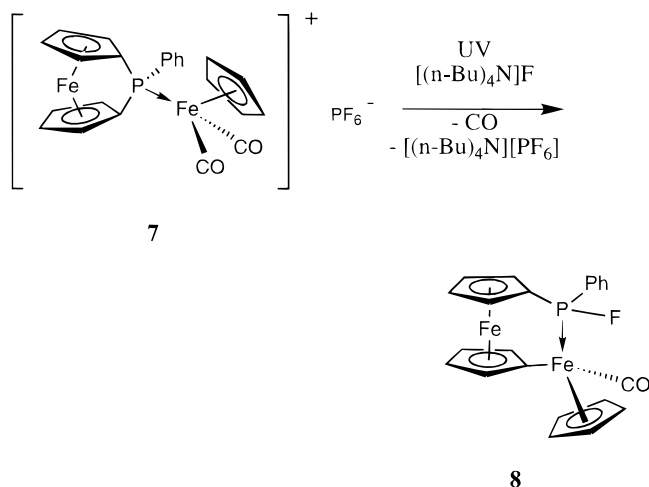
via living anionic ROP of **3a**.<sup>14,15</sup> To date, no transition-metal-catalyzed routes have been reported, as all known catalysts simply coordinate to the P(III) center of **3a** without leading to ROP.

The interesting chemistry of compound **3a** has been explored by a number of groups, particularly by Seyferth *et al.*, who were able to coordinate a number of different moieties to the phosphorus, including sulfur to give **5a** and Fe(CO)<sub>4</sub> moieties to give **6**.<sup>16</sup>

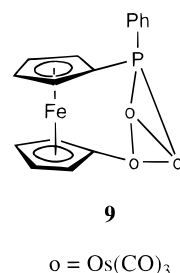


Nakazawa, Miyoshi, *et al.* found that upon coordination of Fe( $\eta^5$ -C<sub>5</sub>H<sub>5</sub>)(CO)<sub>2</sub> to the bridging phosphorus atom (to give **7**), irradiation with UV light led to ring-

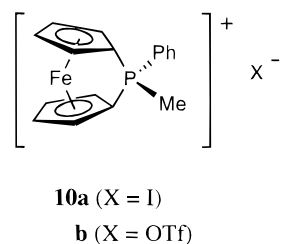
opening and formation of **8** in the presence of [(*n*-Bu)<sub>4</sub>N]F with the concurrent loss of CO and formation of [(*n*-Bu)<sub>4</sub>N][PF<sub>6</sub>].<sup>17</sup>



Ring-opening of **3a** in the presence of a transition metal has also been reported by Cullen *et al.*<sup>18</sup> This involved the thermal reaction (125 °C) of **3a** with Os<sub>3</sub>(CO)<sub>12</sub>, which resulted in the major product Os<sub>3</sub>(CO)<sub>9</sub>[ $\mu_3$ -(C<sub>5</sub>H<sub>4</sub>PPh)Fe(C<sub>5</sub>H<sub>4</sub>)] (**9**).



Another potentially interesting tetracoordinate phosphorus-bridged [1]ferrocenophane, **10a**, was described by Seyferth *et al.*<sup>16</sup> This compound was synthesized by



the reaction of **3a** with MeI. Although the compound was characterized by <sup>31</sup>P and <sup>1</sup>H NMR, no crystals suitable for X-ray analysis could be grown and the compound was reported to be unstable in solution.

In this paper we report on our studies of the ROP behavior, particularly by transition-metal catalysts, of several tetracoordinate phosphorus-bridged [1]ferrocenophanes (**5a**, **6**, and **7**) as well as our preparation of

- (3) Manners, I. *Angew. Chem., Int. Ed. Engl.* **1996**, *35*, 1602.  
 (4) Foucher, D. A.; Tang, B.-Z.; Manners, I. *J. Am. Chem. Soc.* **1992**, *114*, 6246.  
 (5) Manners, I. *Adv. Organomet. Chem.* **1995**, *37*, 131.  
 (6) Manners, I. *Can. J. Chem.* **1998**, *76*, 371.  
 (7) Rulkens, R.; Lough, A. J.; Manners, I. *Angew. Chem., Int. Ed. Engl.* **1996**, *35*, 1805.  
 (8) Pudelski, J. K.; Gates, D. P.; Rulkens, R.; Lough, A. J.; Manners, I. *Angew. Chem., Int. Ed. Engl.* **1995**, *34*, 1506.  
 (9) Braunschweig, H.; Dirk, R.; Müller, M.; Nguyen, P.; Resendes, R.; Gates, D. P.; Manners, I. *Angew. Chem., Int. Ed. Engl.* **1997**, *36*, 2338.  
 (10) Honeyman, C. H.; Foucher, D. A.; Dahmen, F. Y.; Rulkens, R.; Lough, A. J.; Manners, I. *Organometallics* **1995**, *14*, 5503. Note that poly(ferrocenylphosphine) **4a** has been previously reported by a condensation route: Withers, H. P.; Seyferth, D.; Fellmann, J. D.; Garrou, P. E.; Martin, S. *Organometallics* **1982**, *1*, 1283.  
 (11) For the work of other groups on poly(ferrocenylsilanes) see: (a) Nguyen, M. T.; Diaz, A. F.; Dement'ev, V. V.; Pannell, K. H. *Chem. Mater.* **1993**, *5*, 1389. (b) Hmyene, M.; Yasser, A.; Escorne, M.; Percheron-Guegan, A.; Garnier, F. *Adv. Mater.* **1994**, *6*, 564. (c) Reddy, N. P.; Yamashita, H.; Tanaka, M. *J. Chem. Soc., Chem. Commun.* **1995**, 2263. (d) Barlow, S.; Rohl, A. L.; Shi, S.; Freeman, C. M.; O'Hare, D. *J. Am. Chem. Soc.* **1996**, *118*, 7578. (e) Park, J.; Seo, Y.; Cho, S.; Whang, D.; Kim, K.; Chang, T. *J. Organomet. Chem.* **1995**, *489*, 23.  
 (12) (a) Ni, Y.; Rulkens, R.; Manners, I. *J. Am. Chem. Soc.* **1996**, *118*, 4102. (b) Massey, J. A.; Power, K. N.; Winnik, M.; Manners, I. *J. Am. Chem. Soc.* **1998**, *120*, 9533. (c) Massey, J. A.; Power, K. N.; Winnik, M.; Manners, I. *Adv. Mater.* **1998**, *10*, 1559.  
 (13) (a) Ni, Y.; Rulkens, R.; Pudelski, J. K.; Manners, I. *Makromol. Chem. Rapid Commun.* **1995**, *16*, 637. (b) Gómez-Elipé, P.; Resendes, R.; Macdonald, P. M.; Manners, I. *J. Am. Chem. Soc.* **1998**, *120*, 8348.  
 (14) Honeyman, C. H.; Peckham, T. J.; Massey, J. A.; Manners, I. *J. Chem. Soc., Chem. Commun.* **1996**, 2589.  
 (15) Peckham, T. J.; Massey, J. A.; Honeyman, C. H.; Manners, I. *Macromolecules*, in press.  
 (16) Seyferth, D.; Withers, H. P. *Organometallics* **1982**, *1*, 1275. Recently Brinzinger and co-workers have reported phosphonium-bridged group 1 and 2 bis(cyclopentadienyl) complexes: Leyser, N.; Schmidt, K.; Brintzinger, H. H. *Organometallics* **1998**, *17*, 2155.

(17) Mizuta, T.; Yamasaki, T.; Nakazawa, H.; Miyoshi, K. *Organometallics* **1996**, *15*, 1093.

(18) Cullen, W. R.; Retting, S. J.; Zheng, T. C. *J. Organomet. Chem.* **1993**, *452*, 97.

a more stable analogue of **10a**, with a triflate counterion, and our ROP studies on this species.

## Results and Discussion

**Attempted Transition-Metal-Catalyzed ROP of [1]Ferrocenophanes **5a**, **6**, and **7**.** Although thermal ROP of phosphorus-bridged [1]ferrocenophanes has been reported previously by our group, mainly bis(trimethylsilyl) sulfide and low-molecular-weight material were isolated from an otherwise insoluble product from the thermal ROP for **5b**.<sup>10</sup> In light of this evidence, it was thought that an attempt to thermally ROP **5a** would lead to the formation of H<sub>2</sub>S, a possible safety hazard. As expected, no formation of polymer was observed on an attempted transition-metal-catalyzed polymerization in solution using either Pt(II) (PtCl<sub>2</sub>) or Pt(0) (Karstedt's catalyst) initiators.

Similarly, the thermal ROPs of **6** and **7** were avoided due to the possibility for the release of CO. Transition-metal-catalyzed experiments with both PtCl<sub>2</sub> and Karstedt's catalyst also did not lead to the formation of polymer in the case of either compound. We then decided to investigate the ROP behavior of phosphonium-bridged [1]ferrocenophanes.

**Synthesis and Characterization of **10b**.** As mentioned above, Seyferth reported that the treatment of **3a** with MeI led to the formation of **10a** which was determined to be unstable in solution.<sup>16</sup> In light of the sensitivity of **3a** to nucleophiles, we attempted to synthesize a derivative of **10a** with a less nucleophilic counteranion.

Our choice of methyl triflate as a methylating reagent proved to be successful. Compound **10b** was isolated in high yield and characterized by <sup>1</sup>H, <sup>13</sup>C, <sup>19</sup>F, and <sup>31</sup>P NMR as well as elemental analysis, which were all consistent with the proposed structure. The compound was also found to be stable in solution under N<sub>2</sub> and could be isolated as dark red microcrystals suitable for single-crystal X-ray analysis by recrystallization from a THF/CH<sub>2</sub>Cl<sub>2</sub> mixture. Additionally, the compound was found to be stable to air and moisture in the solid state but decomposed slowly over several hours in solution.

An examination of the NMR data revealed some interesting features. The <sup>1</sup>H NMR spectrum of **10b** has four distinct resonances due to four inequivalent cyclopentadienyl (Cp) protons. This is in contrast to the corresponding spectrum of **3a**, in which only three resonances are seen in the Cp region. The phenyl region for **10b** is also more distinct than that for **3a** and, in addition, displays a coupling pattern consistent with a monosubstituted benzene ring attached to a phosphonium center. Perhaps most revealing in the <sup>1</sup>H NMR spectrum is the doublet at 2.66 ppm due to a methyl group attached directly to phosphorus (<sup>2</sup>J<sub>PH</sub> = 13.9 Hz). The resonance at 37.5 ppm in the <sup>31</sup>P NMR spectrum is in agreement with a tetrasubstituted phosphorus center (*cf.* the resonance for **3a** at 13 ppm) and has almost the same shift (37 ppm) found for **10a**.<sup>16</sup> The data provided by the <sup>13</sup>C NMR spectrum is similarly consistent with the strained [1]ferrocenophane structure proposed for **10b**, especially the dramatically upfield-shifted ipso carbon of the cyclopentadienyl rings at 4.2 ppm.<sup>5</sup>

**Single-Crystal X-ray Diffraction Study of **10b**.** Crystals of **10b** suitable for a single-crystal X-ray

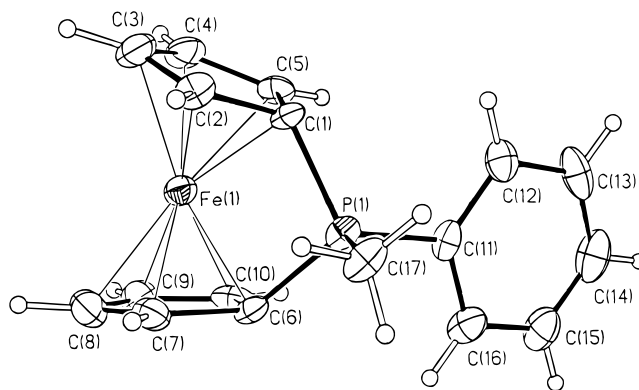


**Figure 1.** Molecular structure of **10b** (vibrational ellipsoids at 25% probability level).

**Table 1. Summary of Crystal Data and Intensity Collection Parameters for **10b****

empirical formula	C <sub>18.5</sub> H <sub>16</sub> ClF <sub>3</sub> FeO <sub>3</sub> PS
fw	497.64
wavelength (Å)	0.710 73
cryst syst	monoclinic
space group	C2/c
a (Å)	23.380(1)
b (Å)	13.339(1)
c (Å)	12.715(1)
α (deg)	90
β (deg)	91.79(1)
γ (deg)	90
V (Å <sup>3</sup> )	3963.4(14)
Z	8
ρ(calcd) (g cm <sup>-3</sup> )	1.668
abs coeff (mm <sup>-1</sup> )	1.127
F(000)	2016
cryst size (mm)	0.18 × 0.04 × 0.03
θ range for data collectn (deg)	2.40–20.90
no. of rflns collected	7331
no. of indep rflns	2052 (R <sub>int</sub> = 0.1013)
no. of data/restraints/params	2052/0/268
goodness of fit on F <sup>2</sup>	1.077
final R indices [I > 2σ(I)]	R1 = 0.0569, wR2 = 0.1421
R indices (all data)	R1 = 0.1023, wR2 = 0.1640
extinction coeff	0.0007(2)
largest diff peak and hole (e Å <sup>-3</sup> )	0.510 and -0.411

diffraction study were obtained from a THF/CH<sub>2</sub>Cl<sub>2</sub> mixture at -30 °C. Only very small crystals of the sample (0.18 × 0.04 × 0.03 mm) were available for data collection. Data were collected on a Nonius Kappa-CCD using graphite-monochromated Mo Kα radiation (λ = 0.710 73 Å). A total of 180 frames, of 1° rotations of φ, were exposed for 90 s each. There were no measurable data higher than 21° in θ. The data were integrated and scaled using the DENZO package.<sup>19</sup> The structure was solved and refined using the SHELXTL/PC package.<sup>20</sup> Refinement was by full-matrix least squares on F<sup>2</sup> using all data (negative intensities included). The weighting scheme was w = 1/[σ<sup>2</sup>(F<sub>o</sub><sup>2</sup>) + (0.0699)<sup>2</sup> + 25.07P], where P = (F<sub>o</sub><sup>2</sup> + 2F<sub>c</sub><sup>2</sup>)/3. Hydrogen atoms were included in calculated positions. A view of the molecular structure is shown in Figure 1. Table 2 gives selected structural data for **10b** as well as for related phosphorus-bridged [1]ferrocenophanes. The angles α, β, θ, and δ are defined in Figure 2. A summary of the crystal data and collection parameters can be found in Table 1. A table of the fractional coordinates is given in the Supporting Infor-

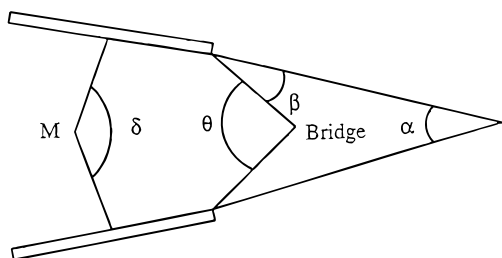
(19) DENZO-SMN; Nonius Co., Delft, Holland, 1997.

(20) Sheldrick, G. M. SHELXTL(NT)PC; Siemens Analytical X-ray Instruments Inc., Madison, WI, 1994.

**Table 2. Selected Structural Parameters for 10b and Related Phosphorus-Bridged [1]Ferrocenophanes, with Esd's in Parentheses (Where Available)**

	compd				
	3a	3a <sup>a</sup>	3c	5b	10b
Fe–P dist (Å)	2.774(3)	2.784(2)	2.755(5)	2.688(2)	2.577(3)
Fe displacement (Å)		0.291(7)	0.277(8)	0.259(2)	0.232(9)
P–C (C <sub>p</sub> ipso) (av) (Å)	1.842(13)	1.857(8)	1.841(20)	1.812(5)	1.772(10)
ring tilt $\alpha$ (deg)	26.7	27.5(6)	27.0(6)	25.3(3)	24.4(5)
$\beta$ (av) (deg)	32.5	32.0(3)	31.9(7)	35.0(4)	37.9(4)
$\theta$ (av) (deg)	90.6(3)	95.7(4)	90.1(7)	95.0(2)	99.8(4)
$\delta$ (av) (deg)	159.8	159.5(3)	160.4(6)	161.8(2)	163.6(4)
ref	43	10	10	10	this work

<sup>a</sup> Trimethylsilyl substituents in the 3,3'-positions on the cyclopentadienyl rings.

**Figure 2.** Distortions in group 8 metallocenophanes: defining angles  $\alpha$ ,  $\beta$ ,  $\theta$ , and  $\delta$ .**Table 3. Bond Lengths (Å) for 10b with Esd's in Parentheses**

Fe(1)–C(6)	1.968(8)	Fe(1)–C(10)	1.979(9)
Fe(1)–C(1)	1.979(9)	Fe(1)–C(7)	1.997(9)
Fe(1)–C(2)	2.015(9)	Fe(1)–C(5)	2.020(9)
Fe(1)–C(3)	2.062(9)	Fe(1)–C(4)	2.062(9)
Fe(1)–C(8)	2.083(11)	Fe(1)–C(9)	2.090(10)
Fe(1)–P(1)	2.577(3)	P(1)–C(17)	1.765(9)
P(1)–C(6)	1.768(9)	P(1)–C(6)	1.777(9)
P(1)–C(11)	1.785(9)	C(1)–C(2)	1.432(12)
C(1)–C(5)	1.437(12)	C(2)–C(3)	1.388(13)
C(3)–C(4)	1.389(13)	C(4)–C(5)	1.409(13)
C(6)–C(10)	1.465(12)	C(6)–C(7)	1.465(12)
C(7)–C(8)	1.384(13)	C(8)–C(9)	1.414(14)
C(9)–C(10)	1.395(13)	C(11)–C(12)	1.374(13)
C(11)–C(16)	1.380(13)	C(12)–C(13)	1.405(14)
C(13)–C(14)	1.36(2)	C(14)–C(15)	1.35(2)
C(15)–C(16)	1.372(13)	C(1S)–F(3)	1.246(14)
C(1S)–F(1)	1.311(13)	C(1S)–F(2)	1.319(14)
C(1S)–S(1)	1.770(13)	O(2)–S(1)	1.413(7)
S(1)–O(1)	1.371(9)	S(1)–O(3)	1.420(9)
C(2S)–Cl(1)	1.706(12)	C(2S)–Cl(1) #1	1.706(12)

**Table 4. Selected Bond Angles for 10b with Esd's in Parentheses**

C(1)–P(1)–C(6)	99.8(4)	C(2)–C(1)–P(1)	117.4(7)
C(1)–P(1)–C(11)	109.4(4)	C(5)–C(1)–P(1)	118.5(6)
C(6)–P(1)–C(11)	110.4(4)	C(2)–C(1)–C(5)	107.2(8)
C(17)–P(1)–C(1)	112.2(4)	C(2)–C(3)–C(4)	110.5(9)
C(17)–P(1)–C(6)	111.5(4)	C(3)–C(2)–C(1)	106.9(8)
C(17)–P(1)–C(11)	112.9(4)		

mation; bond lengths and selected angles are found in Tables 3 and 4, respectively.

The single-crystal X-ray diffraction study agrees with the structure assigned to **10b**. Disordered CH<sub>2</sub>Cl<sub>2</sub> molecules were found to be included within the unit cell. However, no significant interaction was found between the ferrocenophane moiety and either CH<sub>2</sub>Cl<sub>2</sub> or the triflate counterion. In comparison to other phosphorus-bridged [1]ferrocenophanes, **10b** possesses the smallest tilt angle yet known for such a species (24.4(5)°). This value is even smaller than for the phosphorus(V)-bridged species **5b** (25.3(3)°).<sup>10</sup> Perhaps most interesting to note is the very short Fe–P distance of 2.577(3) Å,

shorter even than that for **5b** (2.688(2) Å). This may indicate that there is a greater iron–phosphorus interaction occurring in this compound than in previous examples of phosphorus-bridged [1]ferrocenophanes. This is not particularly surprising, as the electrophilicity of the phosphorus atom in **10b** is probably greater than in any of the other examples and thus possibly a stronger dative bond from the relatively electron-rich iron atom exists in this situation. This may be partially responsible for the large  $\beta$  angle for this compound (37.9(4)°). However, it should also be noted that the ipso Cp carbon–phosphorus bond length is also shorter in **10b** (1.772(10) Å) than in the other examples. This might also at least be partially responsible for the shorter Fe–P distance as well as the larger  $\beta$  angle.

In comparison to other phosphonium compounds, the geometry and bond lengths in the case of **10b** are fairly typical with expected values in the area of 1.78–1.83 Å for P–C(sp<sup>2</sup>) bonds and bond angles of 107–114°. The P–C(sp<sup>3</sup>) bond length (1.765(9) Å) is somewhat shorter than the expected value (1.80 Å), and the  $\theta$  angle of 99.8(4)° is also smaller than expected for a phosphonium compound, although it is a larger angle than is found for other phosphorus-bridged [1]ferrocenophanes. These results may be the effect of the strained nature of this compound. In the case of the  $\theta$  angle, this is probably due to the combined effect of the shorter P–C (Cp-*ipso*) bond lengths and the possible dative interaction between iron and phosphorus.

**Electronic Spectrum and Electrochemical Behavior of 10b.** The electronic structure of **10b** was examined by UV/vis spectroscopy. The band II  $\lambda_{\text{max}}$  value of 484 nm (in THF; the value in DMF is the same) is significantly blue-shifted in comparison to the value of 498 nm (in hexanes) for **3a**. Both values are much higher than was found for ferrocene (440 nm in hexanes). This red shift has been observed previously in other strained [1]ferrocenophanes and has been at least partially attributed to the tilting of the cyclopentadienyl rings from the planarity of ferrocene and unstrained, bridged ferrocenophanes. EHMO calculations on silicon- and sulfur-bridged [1]ferrocenophanes as well as on ferrocene in which the rings are tilted by the same angle (31.05°) as for the sulfur-bridged [1]ferrocenophane illustrate that the HOMO–LUMO gap grows smaller as the tilt angle is increased due to a lowering of the LUMO energy level.<sup>22,23</sup> The smaller tilt angle of **10b**

(21) Cristau, H. J.; Plénat, F. In *The Chemistry of Organophosphorus Compounds*; Hartley, F. R., Ed.; Wiley: Toronto, 1994; Vol. 3, p 45.

(22) Barlow, S. D.; M. J.; Dijkstra, T.; Green, J. C.; O'Hare, D.; Whittingham, C.; Wynn, H. H.; Gates, D. P.; Manners, I.; Nelson, J. M.; Pudelski, J. K. *Organometallics* **1998**, *17*, 2113.

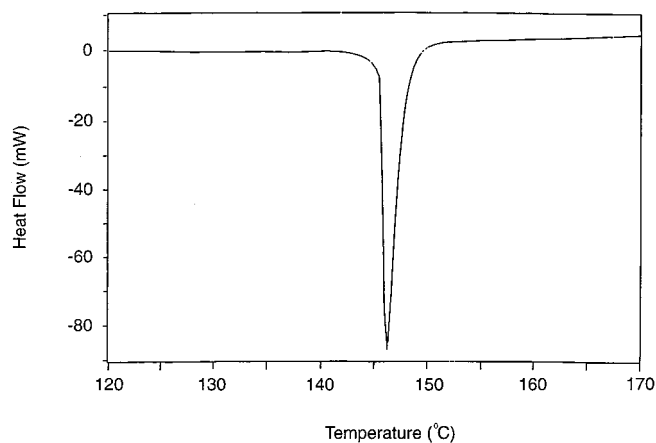


**Figure 3.** DSC thermogram of **10b**.

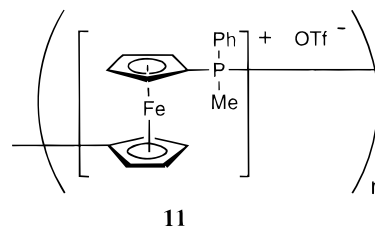
(24.5°) in comparison to **3a** (26.7°) would appear to agree with these calculations. However, it should also be noted that the iron–phosphorus distance in **10b** (2.577 Å) is significantly shorter than in **3a** (2.774 Å) and there may be also some degree of iron–phosphorus interaction which is influencing the size of the HOMO–LUMO gap in addition to the difference in tilt angle. Some evidence for a dative iron–bridging element bond in ferrocenophanes has been provided in the past by  $^{57}\text{Fe}$  Mössbauer spectroscopy.<sup>22,24</sup>

Cyclic voltammetry was used to examine the electrochemical behavior of **10b**. Analysis (in  $\text{CH}_2\text{Cl}_2$ ) revealed one irreversible oxidation wave at ( $E_p(\text{ox})$ ) +0.72 V (vs ferrocene) at a scan rate of 250 mV/s. For comparison, the  $E_{1/2}$  value for **1** ( $\text{ER}_x = \text{SiMe}_2$ ) is only 0.00 V. This suggests that the phosphonium center exhibits a strong electron-withdrawing effect on the iron center. The value of +0.72 V also represents the highest oxidation potential found to date for a [1]ferrocenophane. Measurements were also carried out in DMF. Again, there was only one irreversible wave ( $E_p(\text{ox}) = +0.26$  V vs ferrocene) at a scan rate of 250 mV s<sup>-1</sup> with the smaller difference in oxidation potential versus ferrocene probably attributable to the donating nature of the solvent (DMF). In contrast to the scan carried out in  $\text{CH}_2\text{Cl}_2$  in which no other compound could be observed other than that for **10b**, the second scan of the solution of **10b** in DMF revealed that one or more uncharacterized products had been formed during the first scan which then subsequently underwent two partially reversible oxidation waves at -0.41 and -0.10 V (the wave due to **10b** was still visible) at a scan rate of 250 mV s<sup>-1</sup>.  $^{31}\text{P}$  NMR and  $^1\text{H}$  NMR analyses of the solution before and after the cyclic voltammetric experiment indicated the presence of only **10b**. These results, as expected, indicated that the compounds formed during the experiment are formed only in the vicinity of the electrode and not in the bulk solution, in which **10b** is relatively stable.

**Thermal ROP Behavior of 10b.** The thermal ROP behavior of **10b** was first examined by heating a sample under  $\text{N}_2$  using a DSC (see Figure 3). No melting endotherm was observed. However, a strong exotherm was seen to occur at an onset temperature of 145 °C

upon heating, and no further thermal behavior was seen during the cooling cycle. The energy of this exotherm (enthalpy of polymerization) was found to be  $61 \pm 5$  kJ mol<sup>-1</sup>. By comparison, the enthalpy of polymerization for **3a** was found to be  $68 \pm 5$  kJ mol<sup>-1</sup>.

This behavior led us to believe that thermal ROP of **10b** had taken place, leading to the formation of **11**. This



**11**

ROP experiment was conducted on a preparative scale by heating **10b** in a sealed, evacuated Pyrex tube at 145 °C for 30 min. This led to the formation of a product which was insoluble in ethanol, water, and organic solvents such as  $\text{CH}_2\text{Cl}_2$ , THF, and hexanes but that was soluble in the highly polar solvents DMF, DMSO, methanol, and acetone (the product was found to be unstable in all the solvents but less so in DMF). Analysis of the product by NMR was consistent with a ring-opened structure. In particular, the  $^{31}\text{P}$  NMR spectrum in  $\text{DMSO}-d_6$  showed only one resonance at 23.8 ppm with no sign of any residual monomer ( $\delta$  37.5 ppm). The  $^1\text{H}$  NMR spectrum contained only broad resonances, with none of the definition that had been seen for the monomer but which were nonetheless consistent with the assigned structure. For example, the four resonances in the Cp region of **10b** were reduced to three broad resonances. Similarly, the coupling between the methyl protons and phosphorus could no longer be resolved for **11**. In the case of the  $^{13}\text{C}$  NMR spectrum, the ipso carbon had shifted downfield to 66.5 ppm in comparison to **10b** and was in the region normally associated with Cp carbons in an unstrained system.

**Transition-Metal-Catalyzed ROP Behavior of 10b.** It has been previously noted by other research groups that coordination to the lone pair of the P(III) site or oxidation to P(V) permits facile cleavage of P–C bonds.<sup>17,25–28</sup> With this in mind, we attempted the transition-metal-catalyzed ROP of **10b**. In the presence of approximately 10 mol %  $\text{PtCl}_2$ , **10b** was indeed found to undergo ROP and the polymer formed possessed the same NMR characteristics as that formed via thermal ROP. To our knowledge, this represents the first example of a phosphorus-containing ring that undergoes transition-metal-catalyzed ROP. However, the yields (ca. 56%) were significantly lower than those obtainable via thermal ROP (ca. 70%). We have observed the formation of other products in this reaction which are as of yet unidentified ( $^{31}\text{P}$  NMR spectrum: 25.8 and 25.5 ppm in  $\text{DMSO}-d_6$ ) and appear to be formed in greater amounts with increasing dilution of the reaction solu-

(25) Nakazawa, H.; Matsuoka, Y.; Nakagawa, I.; Miyoshi, K. *Organometallics* **1992**, *11*, 1385.

(26) Arce, A. J.; De Sanctis, Y.; Machado, R.; Capparelli, M. V.; Manzur, J.; Deeming, A. J. *Organometallics* **1995**, *14*, 3592.

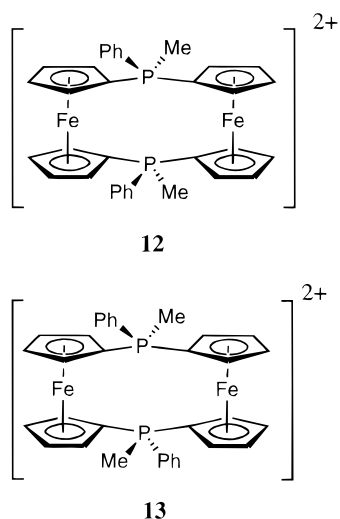
(27) Wicht, D. K.; Kourkine, I. V.; Lew, B. M.; Nthenge, J. M.; Glueck, D. S. *J. Am. Chem. Soc.* **1997**, *119*, 5039.

(28) Carmichael, D.; Hitchcock, P. B.; Nixon, J. F.; Mathey, F.; Pidcock, A. *J. Chem. Soc., Chem. Commun.* **1986**, 762.

(23) Green, J. C. *Chem. Soc. Rev.* **1998**, 263.

(24) Rulkens, R.; Gates, D. P.; Balaishis, D.; Pudelski, J. K.; McIntosh, D. F.; Lough, A. J.; Manners, I. *J. Am. Chem. Soc.* **1997**, *119*, 10976.

tion. In the transition-metal-catalyzed ROP of **1** ( $ER_x = SiMe_2$ ), cyclic dimers analogous to **1** have been isolated from the reaction mixtures.<sup>13</sup> A similar situation may also occur with the thermal and transition-metal-catalyzed ROP of **10b**. The presence of two resonances for the potential dimer may arise from the possibility of *cis* and *trans* isomers, **12** and **13**. Signifi-



cantly, in the case of the transition-metal-catalyzed ROP of **1** ( $ER_x = SiMeCl$ ), a cyclic dimer was proposed as a byproduct of the reaction and the two resonances for this dimer observed in the <sup>29</sup>Si NMR spectrum were attributed to *cis* and *trans* isomers.<sup>29</sup>

In an attempt to synthesize a more generally soluble product, we attempted copolymerizations of **10b** with silicon-bridged [1]ferrocenophanes **1** ( $ER_x = SiMe_2$ ) using both thermal and transition-metal-catalyzed routes. In the case of attempted thermal copolymerizations, only the homopolymer **2** ( $ER_x = SiMe_2$ ) and **11** were isolated. For the transition-metal-catalyzed polymerizations, only **2** ( $ER_x = SiMe_2$ ) and unreacted **10b** were observed. In each case, the absence of copolymerization was shown by the lack of crossover peaks in the <sup>31</sup>P and <sup>1</sup>H NMR spectra of the isolated products.

**Methylation of Poly(ferrocenylphenylphosphine) **14** as an Alternative Route to **11**.** To explore an alternative route to **11**, we studied partial to complete methylation of the well-defined poly(ferrocenylphosphine) **14**, synthesized via anionic ROP of **3a** using *n*-BuLi as an initiator and H<sub>2</sub>O as a termination reagent. Partial methylations ranging from 17% to 50% of phosphorus sites in the polymer were easily achieved by addition of the appropriate amount of MeOTf to a CH<sub>2</sub>Cl<sub>2</sub> solution of **14**. At methylations higher than 50%, it was found that the polymer **15** would precipitate from solution and would not undergo further methylations readily. To achieve 100% methylation, it was necessary to first suspend **14** in MeOTf and to then add CH<sub>2</sub>Cl<sub>2</sub>. This resulted in complete methylation for both the high- ( $n = 100$ ) and low-molecular-weight ( $n = 11$ ) samples of **14**.

Figure 4 illustrates the effect of increasing methylation of **14** on the <sup>31</sup>P NMR spectrum of the polymer.

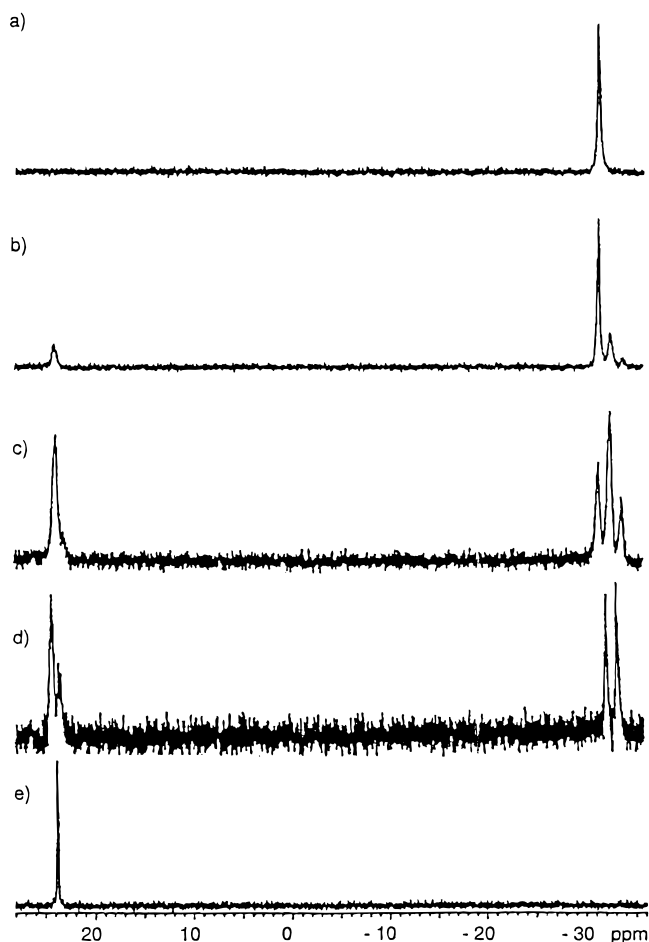
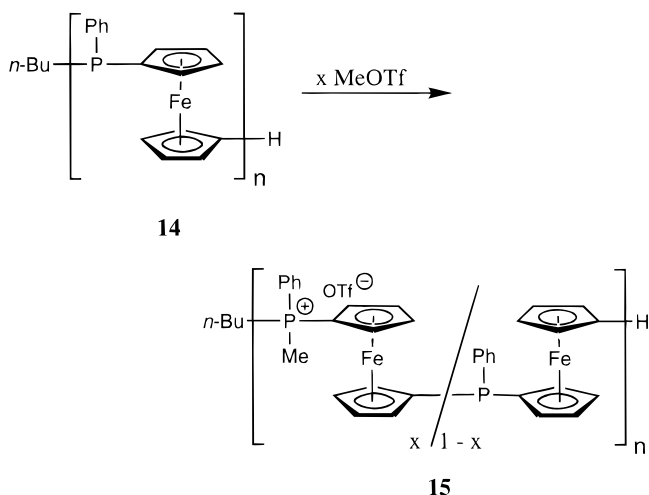


**Figure 4.** <sup>31</sup>P NMR spectra (in CD<sub>2</sub>Cl<sub>2</sub> for a–d and DMSO-*d*<sub>6</sub> for e) of the methylation of polymer **14** ( $n = 100$ ): (a) 0%, (b) 17%, (c) 33%, (d) 50%, and (e) 100% methylation.



Even at a low degree of methylation, the presence of the methyl groups at presumably random phosphorus sites along the polymer main chain leads to different environments that were readily distinguishable by NMR. Thus, unmethylated phosphorus resonances (at ca. -33 ppm) with (i) no Me groups on adjacent P sites ( $-P-fc-P-fc-P-$ ) (where  $fc = (\eta-C_5H_4)_2Fe$  and  $P = PPh$ ), (ii) one Me group on one adjacent P site on either side ( $-P^+-fc-P-fc-P-$ ) (where  $P^+ = PMePh^+$ ), and (iii) Me groups on both of the adjacent P sites ( $-P^+-fc-P-fc-P^+-$ ) were detected. Analogous resonances were

(29) Zechel, D. L.; Hultzs, K. C.; Rulkens, R.; Balaishis, D.; Ni, Y.; Pudelski, J. P.; Lough, A. J.; Manners, I. *Organometallics* **1996**, *15*, 1972.

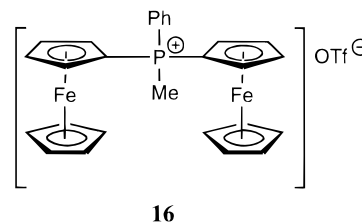
observed for the methylated P sites at *ca.* 24 ppm. At 0% methylation, as expected, only one resonance was detected. At 17% methylation, there is one resonance for the methylated P sites as well as three resonances for the free P sites corresponding to situations i–iii with situation i being the most prevalent and situation iii being the least. However, as the degree of methylation increased, the resonance for  $-P-fc-P-fc-P-$  sites decreased in intensity until, at 50% methylation, only two resonances, due to  $-P^+-fc-P-fc-P-$  and  $-P^+-fc-P-fc-P^+-$  sites, were observed. Also, two resonances due to methylated phosphorus sites can be seen in the spectrum. At 100% methylation, only one resonance is visible with a shift of 23.8 ppm, the same shift found for both the thermal and transition-metal-catalyzed polymerizations of **10b** and, therefore, fully supports our conclusion that **11** can be obtained from **10b** via ROP.

In the case of the complete methylation of the lower ( $n = 11$ ) molecular weight sample of **14**, end groups can also be seen at 26.9 and 24.1 ppm corresponding to the initiated and terminated ends of the polymer chain. End groups can also be detected by  $^1H$  NMR. For all cases, however, no sample would elute from a GPC column using THF for any partially or fully methylated polymers, even after sulfurization of the remaining unreacted P sites and with only 17% methylation. It is unclear at this point in time why this is the case. The reason may involve the presence of interactions between the polymer and the column packing material or simply the decrease in solubility of the methylated polymer in comparison to that of the unmethylated polymer. It should be noted that polymers **4a,b** also do not elute from a GPC column until all the phosphorus sites have been sulfurized.<sup>10</sup>

**Electronic and Electrochemical Properties of 11.** The  $\lambda_{max}$  value obtained for polymer **11** is 452 nm (in DMF), considerably blue-shifted in comparison to the [1]ferrocenophane **10b** ( $\lambda_{max} = 484$  nm in THF and DMF). This is not unusual for these systems and has also been observed for poly(ferrocenylsilanes) and poly(ferrocenylgermanes) relative to their respective monomers.<sup>5</sup> The  $\lambda_{max}$  value of 444 nm (in  $CH_2Cl_2$ ) for polymer **4a** is also blue-shifted relative to **11**. Certainly, in this situation, it is unlikely that this effect is due to a difference in tilt angles for the Cp rings; the rings are probably close to being parallel in the polymer. More likely, it is an example of the effect that the bridging element has upon the HOMO–LUMO gap. In this case, it appears that the presence of phosphonium centers in close proximity to iron leads to a red shift.

Cyclic voltammetry of **11** in DMF revealed the presence of only one redox wave at  $-0.16$  V, which is irreversible at low scan rates ( $I_{red}/I_{ox} = 0.91$  and  $0.82$  at 250 and 100  $mV s^{-1}$ , respectively) but reversible at higher scan rates. The reduction wave is split into two components, which may be a consequence of adsorption to the electrode (Figure 5). The presence of only one wave is unusual and contrasts with the two waves normally detected for poly(ferrocenes) with bridging elements such as silicon, germanium, and phosphorus.<sup>5</sup> However, it is possible that the presence of a cationic phosphonium site as the spacer unit between iron sites decreases the interaction between the metal atoms. Even more unusual is the observation that the  $E_{1/2}$  value

is at a lower oxidation potential than ferrocene. To provide a simple model for **11**, we synthesized compound **16** by reaction of bis(ferrocenyl)phenylphosphine with methyl triflate.



The dimer **16** was found to be soluble in both  $CH_2Cl_2$  and DMF, and thus the electrochemical behavior of this species was examined in each solvent. In  $CH_2Cl_2$ , there were two oxidation waves at  $+0.65$  and  $+0.97$  V and a single reduction wave at  $+0.39$  V (vs ferrocene at 250  $mV s^{-1}$ ) with the shape of the reduction wave possibly due to a two-electron reduction as well as absorption. Similar behavior has been reported for the analogous species with an  $I^-$  counterion.<sup>30</sup> The high oxidation potentials observed for **16** in  $CH_2Cl_2$  are consistent with the high value that was detected for the monomer **10b** in the same solvent.

In DMF, the cyclic voltammogram of **16** revealed only one irreversible oxidation wave at  $-0.14$  V (vs ferrocene at 250  $mV s^{-1}$ ). This is at lower potential than for the monomer **10b**, for which the oxidation wave was found at  $+0.26$  V but is at a similar value for polymer **11** in the same solvent ( $-0.16$  V vs ferrocene at 250  $mV s^{-1}$ ). The unusually low oxidation potentials for dimer **16** and polymer **11** in DMF may be the result of strong solvation of the cationic main chain by the donor solvent. Indeed, on the basis of the solubility properties of polymer **11**, such interactions are probably vital to effect dissolution of the material.

**Thermal Transition Behavior, Thermal Stability, and Morphology of 11.** The thermal transition behavior and the thermal stability of **11** (produced via thermal ROP and transition-metal-catalyzed ROP) were studied by differential scanning calorimetry (DSC) and thermogravimetric analysis (TGA) and compared to those of the unmethylated polymer **14**. The morphologies of the two polymers were examined using wide-angle X-ray scattering (WAXS). By DSC, both **11** and **14** were found to be amorphous, with no evidence for melt transitions for either polymer. However, glass transitions were observed in both cases at 176 and 126  $^{\circ}C$ , for **11** (via thermal ROP) (Figure 6) and **14**,<sup>15</sup> respectively. The higher value for **11** is reasonable, considering that the addition of a methyl group to the backbone of **14** probably reduces the flexibility of the polymer main chain. For comparison, there is an increase in the  $T_g$  value from 9 to 33  $^{\circ}C$  for **2** ( $ER_x = SiHMe$ ) and **2** ( $ER_x = SiMe_2$ ), respectively. Also, the  $T_g$  value for **11** is significantly higher than the value of 54  $^{\circ}C$  for the analogous poly(ferrocenylsilane) **2** ( $R = Me$ ,  $R' = Ph$ ), although the value for **14** is also higher (to date, no analogous silicon-bridged species **2** has been synthesized where  $R = Ph$ ,  $R' = H$ ). However, the triflate counterion no doubt plays a role in the thermal

(30) Kotz, J. C.; Nivert, C. L.; Lieber, J. M.; Reed, R. C. *J. Organomet. Chem.* **1975**, *91*, 87.

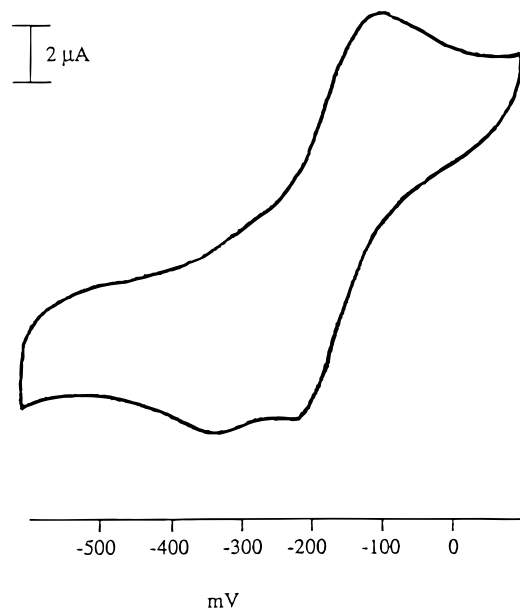


**Figure 5.** Cyclic voltammogram of polymer **11** in DMF at a scan rate of  $250 \text{ mV s}^{-1}$  (referenced vs ferrocene).

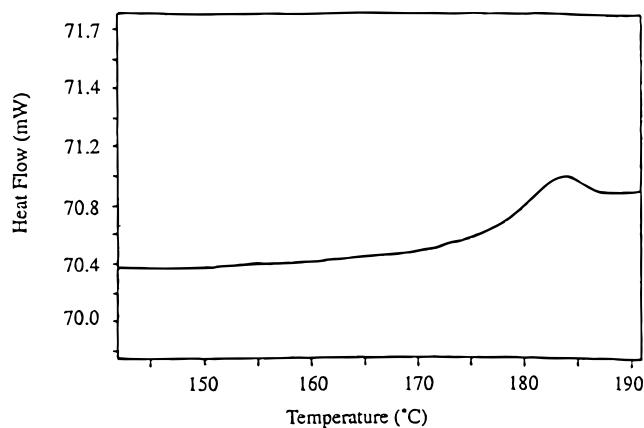


**Figure 6.** DSC thermogram of polymer **11** (produced via thermal ROP).

transition behavior of this polymer as well and may also contribute to its fairly high  $T_g$  value. Interestingly, the  $T_g$  value for **11** derived from the transition-metal-catalyzed ROP of **10b** was found to be  $164 \text{ }^\circ\text{C}$  (see next section). WAXS analysis of these polymers is also consistent with a generally amorphous nature (one broad amorphous halo was detected at  $5.5$  and  $5.2 \text{ \AA}$  for **11** and **14**, respectively).

TGA results reveal similar thermal stabilities for **11** and **14**, and the polymers started to lose weight at  $385$  and  $410 \text{ }^\circ\text{C}$ , respectively. However, the weight loss for **11** is significantly higher than that for **14** with weight losses of  $50\%$  and  $30\%$ , respectively, by  $600 \text{ }^\circ\text{C}$ . This may possibly coincide with the loss of all groups, leaving behind an unsubstituted poly(ferrocenylphosphine) backbone: i.e., loss of phenyl, methyl, and triflate groups from **11**, while **14** only loses phenyl groups.

**Molecular Weight Determination for 11.** We have attempted to determine the molecular weight for **11** by a number of methods, with limited success. In the case of GPC, no polymer was detected using polystyrene sulfonate columns and either *N*-methylpyrrolidinone (NMP) or  $0.2 \text{ M}$  sodium nitrate in methanol/water (75/25) as an elution solvent. As the polymer backbone

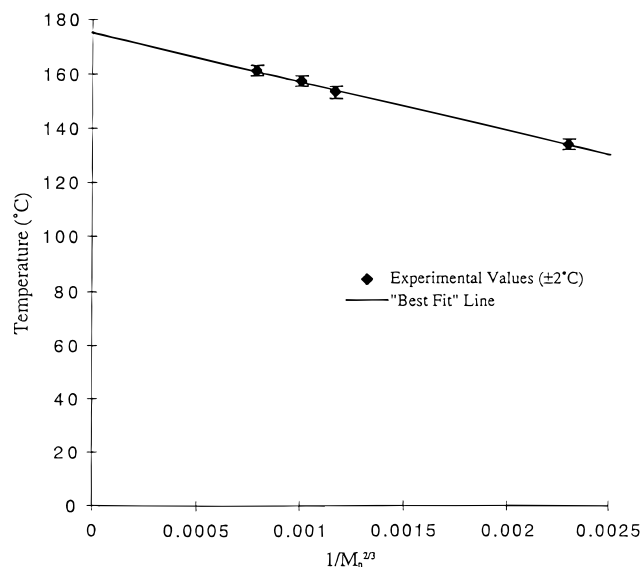


**Figure 7.**  $T_g$  as a function of  $M_n^{-2/3}$  for **11** ( $n = 20\text{--}100$ ) (temperature  $\pm 2 \text{ }^\circ\text{C}$ ).

**Table 5. Thermal Data for Polymer 11 (where  $n$  = Number of Repeat Units)**

$n$	$M_n$	$T_g$ ( $^\circ\text{C}$ )	$\Delta C_p$ (J/(g K))
20	$9.1 \times 10^3$	135	0.18
55	$2.5 \times 10^4$	154	0.18
70	$3.2 \times 10^4$	158	0.19
100	$4.6 \times 10^4$	162	0.19

of **11** is cationic, whereas the column possessed surface negative charges, this is not particularly surprising. In the case of viscometry, the polymer was not found to be stable in DMF or methanol long enough for the relatively time-consuming measurements to be completed and reproducible results to be obtained. Analysis by electrospray mass spectrometry of **11** produced by both thermal transition-metal-catalyzed ROP detected only oligomers (dimer, trimer, and tetramer).

With the problems of polymer stability in mind, dynamic light scattering analyses, which could be performed rapidly, were conducted on samples of **11** obtained via both thermal ROP and transition-metal-catalyzed ROP in methanol. The hydrodynamic radii were in the range of  $30\text{--}45 \text{ nm}$ , which suggested that the compound was polymeric rather than oligomeric in nature. However, due to the instability of the polymer in the solvent as well as the possibility for aggregation, it was not possible to get an accurate value.

As solution methods were hindered by polymer instability in solvents in which the material was soluble, we determined the glass transition temperatures by DSC for a range of samples of polymer **11** of known molecular weight ( $n = 20, 55, 70,$  and  $100$ ) that had been prepared via the 100% methylation of samples of **14** prepared by anionic ROP. The results are shown in Table 5, and the  $T_g$  values were plotted as a function of  $M_n^{-2/3}$  (Figure 7).

We have previously found for polymer **2** (where  $\text{ER}_x = \text{SiMe}_2$ ) that the  $T_g$  value reached a maximum of  $33 \text{ }^\circ\text{C}$  at a length of approximately 90 repeat units<sup>31,32</sup> and

(31) Ni, Y. Z.; Rulkens, R.; Manners, I. *J. Am. Chem. Soc.* **1996**, *118*, 4102.

(32) Lammertink, R. G. H.; Hempenius, M. A.; Manners, I.; Vancso, G. J. *Macromolecules* **1998**, *31*, 795.



the data fit well to the O'Driscoll equation, where  $T_{g,\infty}$  is the glass transition temperature of the polymer with infinite molar mass:<sup>32,33</sup>

$$T_g = T_{g,\infty} - KM_n^{-2/3} \quad (1)$$

Similarly, we found that the data for **11** over the range of 20–100 repeat units fits well to the O'Driscoll equation with a regression coefficient of 0.998. The predicted  $T_{g,\infty}$  value is 175.5 °C. On the basis of these results, this would suggest the  $M_n$  value for **11** derived by transition-metal-catalyzed ROP ( $T_g = 164$  °C) is ca.  $4.6 \times 10^4$ . It is more difficult to determine an approximate molecular weight for the thermal-ROP-derived polymer, as the experimental  $T_g$  value (176 °C) is close to the theoretical  $T_{g,\infty}$  value. The higher  $T_g$  value for the thermal-ROP-derived product in comparison to the value for the transition-metal-catalyzed product does suggest, however, that the former possesses significantly higher molecular weight than the latter. This is not surprising, as the latter precipitates from solution during the polymerization and thus probably cannot reach such a long chain length before becoming completely insoluble in the reaction solvent.

### Summary

The synthesis of a stable, phosphonium-bridged [1]-ferrocenophane (**10b**) has been achieved. The compound was characterized by a variety of spectroscopic techniques as well as by single-crystal X-ray diffraction. In contrast to compounds **5–7**, compound **10b** was found to undergo both thermal and transition-metal-catalyzed ROP. Although a number of phosphonium-containing linear<sup>34–39</sup> and cyclic polymers<sup>40</sup> have been synthesized in the past, the results represent the first synthesis of a phosphonium-containing polymer via ROP as well as the first transition-metal-catalyzed ROP of a phosphorus(III)-containing monomer. The resultant polymer **11** was found to be amorphous and displayed thermal stability similar to that of poly(ferrocenylphosphine) **14**. On the basis of glass transition temperature measurements for a series of samples of polymer **11** of known molecular weight, the number-average molecular weight of **11** produced via transition-metal-catalyzed ROP was ca. 46 000 (ca. 100 repeat units) and the thermally produced polymer was of even higher molecular weight. In contrast to **10b**, a series of tetracoordinate, phosphorus-bridged [1]ferrocenophanes (**5–7**) were found to be resistant to undergo transition-metal-catalyzed ROP in the presence of either Pt(II) or Pt(0) catalysts.

### Experimental Section

**Materials.** All chemicals, unless otherwise noted, were purchased from Aldrich. Compounds **5–7** and bis(ferrocenyl)-

phenylphosphine were synthesized according to the literature.<sup>16,17,41</sup> Samples of polymer **14** were prepared by living anionic polymerization as described previously by our group.<sup>14,15</sup>

**Equipment.** All reactions and manipulations were carried out under an atmosphere of prepurified nitrogen using either Schlenk techniques or an inert-atmosphere glovebox (Vacuum Atmospheres) unless otherwise stated. Solvents were dried by standard methods, distilled, and stored under nitrogen over activated molecular sieves. <sup>1</sup>H NMR spectra (300 MHz), <sup>13</sup>C NMR spectra (75.5 MHz), <sup>19</sup>F NMR spectra (282.3 MHz), and <sup>31</sup>P NMR spectra (121.4 MHz) were recorded on a Varian Gemini 300 spectrometer. <sup>1</sup>H NMR spectra (400 MHz) were also recorded on a Varian Unity 400 spectrometer. Chemical shifts are reported relative to residual protonated solvent (<sup>1</sup>H or <sup>13</sup>C), external H<sub>3</sub>PO<sub>4</sub> (<sup>31</sup>P), or external CFC<sub>3</sub> (<sup>19</sup>F). Melting points and enthalpies of polymerization were obtained with a Perkin-Elmer DSC 7 differential scanning calorimeter operating at a heating rate of 10 °C min<sup>-1</sup> under N<sub>2</sub>. TGA analyses were carried out with a Perkin-Elmer TGA-7 thermogravimetric analyzer under nitrogen at a heating rate of 10 °C min<sup>-1</sup>. UV/vis spectra were recorded on a Perkin-Elmer UV/vis/near-IR Lambda 900 spectrometer in either anhydrous THF or DMF. Elemental analyses were performed by Quantitative Technologies, Inc., Whitehouse, NJ.

Dynamic light scattering experiments were carried out on a wide angle laser light scattering photometer from Brookhaven Instruments Corp. A 5 mW vertically polarized He–Ne laser from Spectra Physics was the light source. The solutions were filtered through disposable 0.2 μm filters from Millipore into glass scattering cells with a diameter of 12.3 mm. The cells were placed into the BI-200SM goniometer and sat in a vat of thermostated toluene which matched the index of refraction of the glass cells. The angle of measurement for the goniometer was 90°. The scattered light was detected by a photomultiplier interfaced to the BI-2030AT digital correlator with 136 channels and measured the correlation function in real time. The instrument was controlled by a 486AT computer. The data were analyzed by software supplied by Brookhaven.

Electrochemical experiments were carried out using a PAR Model 273 potentiostat with a Pt working electrode, a W secondary electrode, and an Ag-wire reference electrode in a Luggin capillary. Polymer solutions were  $1 \times 10^{-3}$  M in CH<sub>2</sub>-Cl<sub>2</sub> with 0.1 M [Bu<sub>4</sub>N][PF<sub>6</sub>] as a supporting electrolyte.

Powder diffraction data were obtained on a Siemens D5000 diffractometer using Ni-filtered Cu Kα ( $\lambda = 1.54178$  Å) radiation. The samples were scanned at step widths of 0.02° with 1.0 s per step in the range of 3–40° in  $2\theta$ . Samples were prepared by spreading the finely ground polymer on grooved glass slides.

**Synthesis of the Methylated Phosphorus-Bridged [1]-Ferrocenophane 10b.** A 1.88 g (6.44 mmol) portion of **3a**<sup>14,42</sup> was dissolved in 50 mL of toluene, giving a dark red solution. A 1.03 g (6.30 mmol) amount of MeOTf was added to this solution dropwise with stirring. A bright red powder was immediately observed to precipitate during the addition. The reaction mixture was stirred for a further 30 min after the addition was complete. The bright orange-red powder was then isolated under N<sub>2</sub> on a filtration frit or under air using a water aspirator and washed with toluene until the washings were colorless. Dark red microcrystals of **10b** could be grown via recrystallization from THF. Yield: 2.54 g (88%). <sup>31</sup>P{<sup>1</sup>H} NMR (CDCl<sub>3</sub>):  $\delta$  37.5 ppm. <sup>19</sup>F NMR (CDCl<sub>3</sub>):  $\delta$  - 78.6 ppm. <sup>13</sup>C NMR (in CDCl<sub>3</sub>):  $\delta$  136.3 (s, para Ph), 131.2 (d, meta Ph, <sup>3</sup>J<sub>PC</sub>

(41) Sollott, G. P.; Mertwoy, H. E.; Portnoy, S.; Snead, J. L. *J. Organomet. Chem.* **1963**, *28*, 1090.

(42) The synthesis of **3a** has been previously described. See: (a) Osborne, A. G.; Whiteley, R. H.; Meads, R. E. *J. Organomet. Chem.* **1980**, *193*, 345. (b) Seyferth, D.; Withers, H. P., Jr. *J. Organomet. Chem.* **1980**, *185*, C1.

(43) Stoeckli-Evans, H.; Osborne, A. G.; Whiteley, R. H. *J. Organomet. Chem.* **1980**, *134*, 91.

(33) O'Driscoll, K.; Sanayei, A. R. *Macromolecules* **1991**, *24*, 4479.

(34) Kanazawa, A.; Ikeda, T.; Endo, T. *J. Polym. Sci.: Polym. Chem.* **1994**, *32*, 641.

(35) Kanazawa, A.; Ikeda, T.; Endo, T. *J. Appl. Polym. Sci.* **1994**, *52*, 1237.

(36) Kanazawa, A.; Ikeda, T.; Endo, T. *J. Appl. Polym. Sci.* **1994**, *52*, 1305.

(37) Kanazawa, A.; Ikeda, T.; Endo, T. *J. Appl. Polym. Sci.* **1994**, *53*, 1245.

(38) Ilzawa, T.; Yamada, Y.; Ogura, Y.; Sato, Y. *J. Polym. Sci.: Polym. Chem.* **1994**, *32*, 2057.

(39) Hughes, I. *Tetrahedron Lett.* **1996**, *37*, 7595.

(40) Seyferth, D.; Masterman, T. C. *Macromolecules* **1995**, *28*, 3055.

= 13 Hz), 130.8 (d, ortho Ph,  $^2J_{PC}$  = 14 Hz), 118.9 (d, ipso Ph,  $^1J_{PC}$  = 90 Hz), 84.5 (d, Cp,  $^3J_{PC}$  = 11 Hz), 83.5 (d, Cp,  $^3J_{PC}$  = 10.4 Hz), 76.4 (d, Cp,  $^2J_{PC}$  = 11.7 Hz), 75.2 (d, Cp,  $^2J_{PC}$  = 14.9 Hz), 11.3 (d, Me,  $^1J_{PC}$  = 55 Hz), 4.2 (d, ipso Cp,  $^1J_{PC}$  = 71.9 Hz) ppm.  $^1H$  NMR (400 MHz, in  $CDCl_3$ ):  $\delta$  8.80 (m, 2H, Ph), 7.89 (m, 1H, Ph), 7.79 (m, 2H, Ph), 5.45 (m, 2H, Cp), 5.02 (m, 2H, Cp), 4.93 (m, 2H, Cp), 4.41 (m, 2H, Cp), 2.66 (d, 3H, Me,  $^2J_{PH}$  = 13.9 Hz) ppm. UV-visible (THF):  $\lambda_{max}$ (band II) 484 nm ( $\epsilon$  = 307  $M^{-1} cm^{-1}$ ). Anal. Calcd for  $C_{18}H_{16}F_3FeO_3PS$ : C, 47.39; H, 3.54. Found: C, 47.11; H, 3.36.

**Thermal ROP of 10b.** A 0.75 g (1.64 mmol) portion of **10b** was sealed in an evacuated Pyrex tube and heated at 145 °C for 30 min. During this time, the contents were observed to undergo a change to a dark red-orange color. After this time, the tube was broken and the polymer washed with  $CH_2Cl_2$ . The product (**11**) was then dried under vacuum and isolated as an orange powder. Yield: 0.65 g (87%).  $^{31}P$  NMR (DMSO- $d_6$ ):  $\delta$  23.8 ppm.  $^{19}F$  NMR (DMSO- $d_6$ ):  $\delta$  -78.2 ppm.  $^{13}C$  NMR (DMSO- $d_6$ ):  $\delta$  134.8 (s, para Ph), 131.6 (d, meta Ph,  $^3J_{PC}$  = 10 Hz), 130.0 (d, ortho Ph,  $^2J_{PC}$  = 13 Hz), 121.7 (d, ipso Ph,  $^1J_{PC}$  = 94 Hz), 76.3–72.8 (Cp, multiplet, broad), 66.5 (ipso Cp,  $^1J_{PC}$  = 102 Hz), 5.2 (d, Me,  $^1J_{PC}$  = 62 Hz) ppm.  $^1H$  NMR (300 MHz, in DMSO- $d_6$ ):  $\delta$  7.85 (broad, 3 H, phenyl), 7.68 (broad, 2 H, Ph), 4.88 (broad, 2 H, Cp), 4.65 (broad, 4 H, Cp), 3.97 (broad, 2 H, Cp), 2.93 (broad, 3H, Me) ppm. UV-visible (DMF):  $\lambda_{max}$ (band II) 452 nm ( $\epsilon$  = 137  $M^{-1} cm^{-1}$ ). Anal. Calcd for  $C_{18}H_{16}F_3FeO_3PS$ : C, 47.39; H, 3.54. Found: C, 46.65; H, 3.55. Electrospray MS:  $m/e$  1676 ([fcPPhMe] $_4$ [OTf] $_3$ , 10%), 1219 ([fcPPhMe] $_3$ [OTf] $_2$ , 100%), 763 ([fcPPhMe] $_2$ [OTf], 10%), 307 ([fcPPhMe] $^+$ , 50%).

**Transition-Metal-Catalyzed ROP of 10b.** A 0.196 g (0.430 mmol) portion of **10b** was dissolved in 5 mL of  $CH_2Cl_2$ . To this solution was added 9 mg (7.9 mol %) of  $PtCl_2$ . The solution was then stirred overnight. A fine light orange powder precipitated out of solution during this time. The precipitate was allowed to settle, and then the solvent was removed via cannulation. The product (**11**) was washed with  $CH_2Cl_2$  and then dried under vacuum.  $^1H$ ,  $^{13}C$ ,  $^{19}F$ , and  $^{31}P$  NMR data were consistent with the same product obtained via thermal ROP. Yield: 0.105 g (54%). Electrospray MS:  $m/e$  1676 ([fcPPhMe] $_4$ [OTf] $_3$ , 10%), 1219 ([fcPPhMe] $_3$ [OTf] $_2$ , 100%), 763 ([fcPPhMe] $_2$ [OTf], 65%), 307 ([fcPPhMe] $^+$ , 100%).

**Partial Methylation of Poly(ferrocenylphenylphosphine) 14 ( $n = 100$ ).** The procedure for various percent methylations of **14** was the same for all samples: (a) 124 mg, (b) 107 mg, or (c) 105 mg of **14** ( $n = 100$ ) ( $M_w$  of sulfurized **14** 38 000,  $M_w/M_n = 1.30$ ) was dissolved in  $CD_2Cl_2$  in a 5 mm NMR tube. To this solution was added, via a microsyringe, (a) 7  $\mu L$ , (b) 14  $\mu L$ , or (c) 21  $\mu L$  of MeOTf.  $^{31}P$  NMR spectra were run. Samples of the solution were then treated with  $S_8$  in an attempt to produce a GPC-analyzable polymer. However, no polymer was found to elute from the Ultrastaygel column using THF as eluent, even for the polymer sample treated with only 7  $\mu L$  of MeOTf. Similarly, a 112 mg sample of **14** ( $n = 100$ ) was treated sequentially with 7  $\mu L$  portions of MeOTf and a  $^{31}P$  NMR spectrum was obtained after each addition. The spectra were essentially the same.

**Complete Methylation of Poly(ferrocenylphenylphosphine) 14 ( $n = 100$ ).** A 65 mg portion of **14** ( $n = 100$ ) ( $M_w$  of sulfurized **14** = 38 000,  $M_w/M_n = 1.30$ ) was suspended in an excess of MeOTf. A 2 mL amount of  $CH_2Cl_2$  was added and the solution stirred for 10 min. The solution was removed and the remaining insoluble material dried under vacuum. The product was analyzed by NMR, and the data were consistent with the structure proposed for the products of thermal and transition-metal-catalyzed ROP of **10b**.

**Complete Methylation of Poly(ferrocenylphenylphosphine) 14 ( $n = 11$ ).** A 60 mg portion of **14** ( $n = 11$ ) ( $M_w$  of sulfurized **14** 2600,  $M_w/M_n = 1.08$ ) was suspended in an excess of MeOTf. A 2 mL amount of  $CH_2Cl_2$  was added and the solution stirred for 10 min. The mother liquors were removed,

and the remaining insoluble material was dried under vacuum. The product was analyzed by  $^1H$  and  $^{31}P$  NMR, and the data were consistent with the structure proposed for the products of thermal and transition-metal-catalyzed ROP of **10b**. Additionally, end groups were observed by  $^{31}P$  NMR (in DMSO- $d_6$ ) at 26.9 and 24.1 ppm.

**Attempted Thermal Copolymerization of 1 ( $ER_x = SiMe_2$ ) and 10b.** A 100 mg (0.413 mmol) portion of **1** ( $ER_x = SiMe_2$ ) and 53 mg (0.116 mmol) of **10b** were sealed in an evacuated Pyrex tube at 140 °C for 15 min. The THF-soluble fraction of the contents of the tube was dissolved in THF and then precipitated into hexanes. The insoluble and soluble fractions were then dissolved in DMSO- $d_6$  and  $C_6D_6$ , respectively, and analyzed by  $^1H$  and  $^{31}P$  NMR. This analysis revealed only the presence of the respective homopolymers **11** and **2** ( $ER_x = SiMe_2$ ), with no evidence for switching groups.

**Attempted Transition-Metal-Catalyzed Copolymerization of 1 ( $ER_x = SiMe_2$ ) and 10b.** A 193 mg (0.798 mmol) portion of **1** ( $ER_x = SiMe_2$ ) and 109 mg (0.239 mmol) of **10b** were dissolved in 25 mL of  $CH_2Cl_2$ . To this was added 4 mg (6.3 mol %) of  $PtCl_2$ . The reaction mixture was stirred overnight. Analysis as described above revealed only the presence of homopolymers **2** ( $ER_x = SiMe_2$ ) and **11**.

**Attempted Thermal Copolymerization of 1 ( $ER_x = SiMePh$ ) and 10b.** A 151 mg (0.497 mmol) portion of **1** ( $ER_x = SiMePh$ ) and 45 mg (0.099 mmol) of **10b** were sealed in an evacuated Pyrex tube at 140 °C for 15 min. Analysis as described above revealed only the presence of homopolymers **2** ( $ER_x = SiMePh$ ) and **11**.

**Attempted Transition-Metal-Catalyzed Copolymerization of 1 ( $ER_x = SiMePh$ ) and 10b.** A 160 mg (0.526 mmol) portion of **1** ( $ER_x = SiMePh$ ) and 50 mg (0.110 mmol) of **10b** were dissolved in 25 mL of  $CH_2Cl_2$ . To this was added 4 mg (13.6 mol %) of  $PtCl_2$ . The reaction mixture was stirred overnight. Examination of the products by  $^1H$  and  $^{31}P$  NMR showed evidence only for homopolymer **2** ( $ER_x = SiMePh$ ) and unreacted **10b**.

**Attempted Transition-Metal-Catalyzed Copolymerization of 5a.** A 60 mg portion (0.19 mmol) of **5a** was dissolved in 0.7 mL of  $C_6D_6$  in a 5 mm NMR tube. To this solution was added 8 mol % of  $PtCl_2$ . The contents of the tube were shaken at intermittent intervals over 24 h. No change in the  $^{31}P$  NMR spectrum was observed during this time. The contents were also heated at 60 °C overnight. No changes were observed by  $^{31}P$  NMR.

**Attempted Transition-Metal-Catalyzed ROP of 6.** A 60 mg (0.13 mmol) portion of **6** was dissolved in 0.7 mL of  $C_6D_6$  in a 5 mm NMR tube. To this solution was added 8 mol % of  $PtCl_2$ . The contents of the tube were shaken at intermittent intervals over 24 h. No change in the  $^{31}P$  NMR spectrum was observed during this time. The contents were also heated at 60 °C overnight. No changes were observed by  $^{31}P$  NMR.

**Synthesis of Model Compound 16.** A 0.362 g (0.757 mmol) portion of bis(ferrocenyl)phenylphosphine was dissolved in 5 mL of toluene. To this stirred solution was added 0.128 g (0.780 mmol) of MeOTf. A reddish orange oil was immediately observed to precipitate from solution. The solution was removed by decantation. The oil was dissolved in  $CH_2Cl_2$  and precipitated into hexanes. The solution was removed by decantation. The product was dried overnight under vacuum and isolated as a reddish orange semisolid. Yield: 0.406 g (84%).  $^{31}P\{^1H\}$  NMR ( $CDCl_3$ ):  $\delta$  24.8 ppm.  $^{19}F$  NMR ( $CDCl_3$ ):  $\delta$  -78.5 ppm.  $^{13}C$  NMR (in  $CDCl_3$ ):  $\delta$  134.4 (s, para Ph), 131.6 (d, meta Ph,  $^3J_{PC}$  = 9 Hz), 129.9 (d, ortho Ph,  $^2J_{PC}$  = 12 Hz), 122.9 (d, ipso Ph,  $^1J_{PC}$  = 92 Hz), 74.3 (d, Cp,  $^3J_{PC}$  = 9.9 Hz), 73.9 (d, Cp,  $^3J_{PC}$  = 9.7 Hz), 72.6 (d, Cp,  $^2J_{PC}$  = 12.6 Hz), 71.8 (d, Cp,  $^2J_{PC}$  = 13.5 Hz), 70.8 (s, Cp), 63.6 (d, ipso Cp,  $^1J_{PC}$  = 105 Hz), 10.8 (d, Me,  $^1J_{PC}$  = 64 Hz) ppm.  $^1H$  NMR (400 MHz, in  $CDCl_3$ ):  $\delta$  7.5–7.9 (m, 5 H, Ph), 4.79 (m, 2H, Cp), 4.73 (m, 2H, Cp), 4.63 (m, 2 H, Cp), 4.41 (m, 2 H, Cp), 4.20 (s, 10 H,

Cp), 2.93 (d, 3 H, Me,  $^2J_{\text{PH}} = 13.9$  Hz) ppm. Anal. Calcd for  $\text{C}_{28}\text{H}_{26}\text{F}_3\text{Fe}_2\text{O}_3\text{PS}$ : C, 52.37; H, 4.08. Found: C, 52.62; H, 4.20.

**Acknowledgment.** This work was funded by the Natural Sciences and Engineering Research Council (NSERC). T.J.P. thanks the NSERC for a graduate scholarship, and I.M. thanks the Alfred P. Sloan Foundation for a Research Fellowship (1994–1998), the NSERC for an E. W. R. Steacie Fellowship (1997–1998), and the University of Toronto for a McLean Fellowship. We also thank Jason Massey for performing dynamic

light scattering studies on polymer **11** and Mark MacLachlan for obtaining WAXS profiles of polymers **11** and **14**. We are also grateful to Kristina Barr for help in the preparation of the manuscript.

**Supporting Information Available:** A table giving positional parameters and isotropic thermal parameters for **10b**. This material is available free of charge via the Internet at <http://pubs.acs.org>.

OM980696T